PLOS | ONE

RESEARCH ARTICLE

Absolute Cerebral Blood Flow Infarction Threshold for 3-Hour Ischemia Time Determined with CT Perfusion and ^{18}F-FFMZ-PET Imaging in a Porcine Model of Cerebral Ischemia

Eric A. Wright[1,2,3☯]*, Christopher D. d'Esterre[4☯], Laura B. Morrison[3☯], Neil Cockburn[3‡], Michael Kovacs[1,3,5‡], Ting-Yim Lee[1,2,3,5,6☯]

1 Department of Medical Biophysics, Western University, London, Ontario, Canada, **2** Robarts Research Institute, Western University, London, Ontario, Canada, **3** Lawson Imaging, Lawson Health Research Institute, London, Ontario, Canada, **4** Department of Radiology, Foothills Medical Center, University of Calgary, Calgary, Alberta, Canada, **5** Department of Medical Imaging, Western University, London, Ontario, Canada, **6** Department of Oncology, Western University, London, Ontario, Canada

☯ These authors contributed equally to this work.
‡ These authors also contributed equally to this work.
* ewrigh32@uwo.ca

Citation: Wright EA, d'Esterre CD, Morrison LB, Cockburn N, Kovacs M, Lee T-Y (2016) Absolute Cerebral Blood Flow Infarction Threshold for 3-Hour Ischemia Time Determined with CT Perfusion and ^{18}F-FFMZ-PET Imaging in a Porcine Model of Cerebral Ischemia. PLoS ONE 11(6): e0158157. doi:10.1371/journal.pone.0158157

Editor: Quan Jiang, Henry Ford Health System, UNITED STATES

Received: January 28, 2016

Accepted: June 10, 2016

Published: June 27, 2016

Data Availability Statement: All relevant data are within the paper and its supporting information files.

Funding: This work was supported by funding from the Canadian Institutes of Health Research (http://www.cihr-irsc.gc.ca/e/193.html) (Grant Number: 246794-MPI, received by TL), the Heart and Stroke Foundation of Canada (http://www.heartandstroke.com/site/c.ikIQLcMWJtE/b.2796497/k.BF8B/Home.htm) (Grant Number: NA6758, received by TL), and the Canada Foundation for Innovation (http://www.innovation.ca/) (Grant Number: 30954, received by

Abstract

CT Perfusion (CTP) derived cerebral blood flow (CBF) thresholds have been proposed as the optimal parameter for distinguishing the infarct core prior to reperfusion. Previous threshold-derivation studies have been limited by uncertainties introduced by infarct expansion between the acute phase of stroke and follow-up imaging, or DWI lesion reversibility. In this study a model is proposed for determining infarction CBF thresholds at 3hr ischemia time by comparing contemporaneously acquired CTP derived CBF maps to ^{18}F-FFMZ-PET imaging, with the objective of deriving a CBF threshold for infarction after 3 hours of ischemia. Endothelin-1 (ET-1) was injected into the brain of Duroc-Cross pigs (n = 11) through a burr hole in the skull. CTP images were acquired 10 and 30 minutes post ET-1 injection and then every 30 minutes for 150 minutes. 370 MBq of ^{18}F-FFMZ was injected ~120 minutes post ET-1 injection and PET images were acquired for 25 minutes starting ~155–180 minutes post ET-1 injection. CBF maps from each CTP acquisition were co-registered and converted into a median CBF map. The median CBF map was co-registered to blood volume maps for vessel exclusion, an average CT image for grey/white matter segmentation, and ^{18}F-FFMZ-PET images for infarct delineation. Logistic regression and ROC analysis were performed on infarcted and non-infarcted pixel CBF values for each animal that developed infarct. Six of the eleven animals developed infarction. The mean CBF value corresponding to the optimal operating point of the ROC curves for the 6 animals was 12.6 ± 2.8 mL·min^{-1}·100g^{-1} for infarction after 3 hours of ischemia. The porcine ET-1 model of cerebral ischemia is easier to implement then

TL). The funders had no role in study design, data collection and analysis, decision to publish, or preparation of the manuscript.

Competing Interests: The authors have read the journal's policy and the authors of this manuscript have the following competing interests: Ting-Yim Lee has a licensing agreement in place with GE Healthcare for the CT Perfusion software used in this study. This does not alter the authors' adherence to PLOS ONE policies on sharing data and materials.

other large animal models of stroke, and performs similarly as long as CBF is monitored using CTP to prevent reperfusion.

Introduction

Both MRI and CT are highly sensitive for infarct core. Generally, CT is used preferentially for stroke diagnosis/prognosis because of availability, cost and speed. Along with non-contrast CT and CT Angiography, CT Perfusion (CTP) is now consistently acquired at many institutes. CTP based time-dependent thresholds for infarct core have been recently derived using data from ischemic stroke patients [1]. These thresholds will have important implications for patient triaging, and will be useful in wake-up and late presenting strokes. Predicting the infarct core evolution could help identify patients who will benefit most from transfer to tertiary centers capable of intra-arterial therapy (IAT), the new standard of care.

However, many threshold derivation studies used follow-up imaging performed 1–7 days after symptom onset to define the infarct core [2–8], introducing uncertainty caused by infarct expansion in the time between admission and follow-up imaging. Furthermore, some of these studies used diffusion weighted imaging (DWI) to define the infarct core [5,6,8]. DWI lesion reversal has been observed in both human and animal ischemic stroke [9,10], though it should be noted that clinical instances of DWI lesion reversal are rare [11], and should not deter anyone from using MRI if it is logistically feasible to acquire in the acute setting.

One alternative, which may circumvent uncertainties caused by infarct expansion and DWI, is to use large animal stroke models to derive time-dependent thresholds for infarction. The logistical complexity of producing and using radiotracers in the clinical acute stroke setting are not a factor, and radiation dose is less of a concern in animal models, so the infarct can be defined using PET imaging with radiolabeled flumazenil (FMZ), or its fluorinated analog, fluoroethylflumazenil (FFMZ). This gold standard method reliably predicts the final infarct and is less prone to false positives then DWI [12]. Furthermore, animal models provide greater control over the time interval between symptom onset and tissue status determination, allowing infarction thresholds to be determined for many different ischemia durations.

Porcine models are more useful then small animal models since the gyrencephalic brain is more similar to a human brain in terms of grey/white matter composition and size [13]. However, the rete mirabelle makes it impossible to use intra-arterial catheter based methods commonly used to initiate cerebral ischemia in small animal models [14]. As a result, most porcine models of stroke rely on complex and invasive surgical procedures to access the middle cerebral artery so a clip or ligature can be applied [15,16]. Using endothelin-1 (ET-1) to cause transient cerebral ischemia does not require complicated surgical procedures and has been well established in rodents and lower primates [17,18]. Application of ET-1 induces changes in CBF that are severe enough to induce infarction, with minimal tissue edema. Recently, the ET-1 method was used in a porcine model of cerebral ischemia [19].

In this study, we presented an ET-1 based porcine model of cerebral ischemia for determining time dependent CBF thresholds for infarction using CTP and ^{18}F-FFMZ-PET imaging, and we determined a CBF threshold for infarction after 3hrs of ischemia.

Methods

Acute Cerebral Ischemia Model

All animal experiments were conducted following the guidelines of the Canadian Council on Animal Care and approved by the Animal Use Subcommittee at the University of Western Ontario (Protocol #2007–050). Duroc Cross Pigs were picked up from a nearby farm on the day of the experiment and were not housed at the laboratory prior to experiments. Out of the 11 animals (average weight 26 ± 5 kg) used in this study, 7 were female and 4 were male. Anesthesia was induced in the animals using 4–5% isoflurane. Anesthesia was maintained by mask with 3–4% isoflurane until intubation. Propofol (16–22 mg/kg) was given IV for intubation. The pig was ventilated (10–15 cc/stroke volume, 20–30 breath per minute) with 2.5–3.5% isoflurane with oxygen and medical air (2:1 medical air to oxygen ratio) for the duration of the experiment. A 22G cephalic vein catheter was placed for injection of CT contrast (Isovue 370) and ^{18}F-FFMZ. One femoral artery was cannulated with a catheter for measuring blood pressure, blood gases (pO_2 and pCO_2), glucose and pH throughout the experiment. In addition heart rate (HR), arterial oxygen saturation (S_aO_2), end-tidal carbon dioxide tension (CO_2), respiration rate (RR) and blood pressure (BP) were continuously monitored (Surgivet). The animal was wrapped in a circulating hot water blanket and rectal temp were monitored continuously throughout the experiment.

A CT scan was done to identify sixteen contiguous 2.5mm thick slices which included the largest coronal sections of the brain, then a baseline CTP study was performed using the procedures outlined in the next section. A target slice location showing the maximal extent of the middle cerebral artery (MCA) territory was selected following the baseline CTP scan. This target slice was marked on the pig's head using the CT scanner laser positioning light, the scalp was incised (silver nitrate sticks used to control bleeding) and a 1-2mm diameter burr hole was made with a Dremel hand tool through the skull. A 27G 1 ¼" long needle attached to a 1mL saline syringe with PE 40 tubing was preloaded with ET-1 and inserted through the burr hole into the brain. An axial CT scan was then acquired to verify that the needle tip is within the cerebral cortex in the target slice. 33μg of ET-1 in 150μL of sterile water was injected at 50 μL/min using an infusion pump. CT Perfusion studies were performed 10 and 30min after the ET-1 injection, and then every 30min for the remainder of the 3hr monitoring period.

Animals were under anesthetic for the entire study to reduce unnecessary animal suffering. If anything seriously detrimental had happened during surgery or scanning, the animal would have been euthanized immediately by intravenous potassium chloride overdose under full deep anesthetic, however there were no serious incidents so early termination of experiments was not necessary. At the conclusion of the experiment animals were euthanized by intravenous potassium chloride overdose under full deep isoflurane anesthetic.

On-line CBF Monitoring with CT Perfusion

CTP studies were acquired on the GE Healthcare Discovery VCT PET/CT scanner using the following protocol: 80kV, 200mA, 16 slices of 2.5mm thickness, 1 scan per second for 60s with a 5s delay from the start of contrast injection (370mg Iodine/mL) at a dosage of 1mL/kg body weight and at an injection rate of 3mL/s. CTP studies were completed at baseline, 10 and 30min post ET-1 injection and then every 30min until 3hr post ischemia. Quantitative CBF maps from each acquired CTP study, calculated within 5min of acquisition, were used to evaluate the perfusion in the ET-1 injection territory. If reperfusion caused CBF to rise above the target range of ~20 $mL \cdot min^{-1} \cdot 100g^{-1}$ (infarction threshold with permanent occlusion [20]), a second dose of ET-1 was injected and perfusion was checked 10min after, before perfusion

monitoring went back to half-hourly intervals. Physiological parameters that have an impact on CBF were monitored throughout the experiment.

^{18}F-FFMZ-PET Imaging for Detecting Cerebral Infarction

FMZ is a selective, high-affinity ligand for the central benzodiazepine receptor of the GABA-A receptor complex [21]. Since cortical neurons have a high concentration of GABA-A receptors, and they are sensitive to early ischemic damage, their activity within the brain is an indicator of neuronal integrity [22]. Previous studies in humans and animals have shown that irreversibly damaged cortical tissue can be detected by decreased binding of carbon-11 (^{11}C) labeled FMZ [21,22]. FFMZ is a fluorinated analogue of flumazenil with similar pharmacokinetics. FFMZ can be labelled with fluorine-18 (^{18}F), which is advantageous because of the longer half-life [23]. Previous studies have shown that PET imaging with ^{18}F-FFMZ can be used to map the activity of GABA-A receptors in the human brain in the same way as ^{11}C-FMZ [24].

^{18}F-FFMZ-PET imaging was performed on the GE Healthcare Discovery VCT PET/CT scanner in the 3D acquisition mode. 370MBq of the tracer was injected 25min before the start of the PET imaging (160min after first ET-1 injection). A CT scan was acquired for attenuation correction. For the PET imaging, 5 frames of 300s duration each (25min total time) were acquired on 47 3.3mm thick slices. The 5 frames were averaged together at all slice locations.

Data Analysis

For consistency, all CTP functional maps were calculated by one author using delay-insensitive deconvolution software (CT Perfusion 5 GE Healthcare, Waukesha, WI) as described previously [25]. For each pig, CBF maps from each CTP imaging time point were co-registered, and the median value of each pixel was found using Matlab, to generate a median CBF map. The median CBF map was then co-registered with the PET images, average images (perfusion-weighted maps) from the baseline CTP study, and blood volume (BV) maps at 10min after the first ET-1 injection. All image registration was manually performed with rigid 3D registration in Analyze 11 (Mayo Clinic, Biomedical Engineering). The average image was used to draw regions of interest (ROIs) covering the cortex on the affected and contralateral sides on all slices containing a defect in ^{18}F-FFMZ uptake. These ROIs were then superimposed onto all other co-registered images. Infarct pixels were identified on PET images as having signal less than the average minus 2 standard deviations from the contralateral ROI. Since GABA-A receptors are located primarily in the grey matter [26], the average image was used to segment out white matter by removing any pixels where the CT number was less than 40 HU. To avoid the influence of large blood vessels on parenchymal perfusion, the BV map was used to exclude blood vessel pixels if they had a BV greater than the average plus 2 standard deviations from the affected side ROI. Additionally, pixels with median CBF greater than 100 $mL \cdot min^{-1} \cdot 100g^{-1}$ were also considered to be blood vessels and excluded from analysis. The remaining infarct and non-infarct grey matter ROIs were then superimposed onto the median CBF map and pixel values were imported into an in-house Matlab program for logistic regression and ROC analysis (Fig 1). This process was repeated for each animal that had a defect in ^{18}F-FFMZ uptake. The CBF values that corresponded to the optimal operating point of the ROC curve [27] for each animal were averaged together to determine the CBF threshold for infarction after 3hrs of ischemia.

Results

6 out of 11 animals had irreversible tissue damage (i.e. uptake defect upon ^{18}F-FFMZ imaging) and were included in the analysis. After removing vessel pixels, the volumes of grey matter

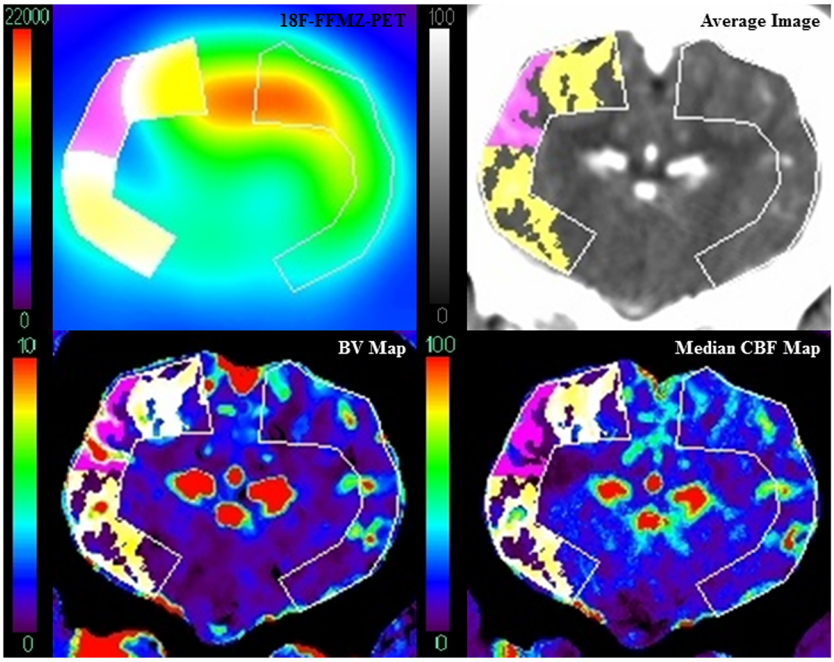

Fig 1. Image Analysis Method. Infarct (pink) was identified on a PET image (top left) acquired 160-185min after ET-1 injection as pixels in the affected side ROI with signal below the infarction threshold derived from the contralateral ROI. Pixels with signal above this threshold were classified as non-infarct (yellow). The average image (top right) was used to segment out white matter. Blood vessels were identified on the BV map (bottom left) using a threshold derived from the affected side ROI (see text). Grey matter, vessel-less infarct and non-infarct ROIs were then superimposed onto the median CBF map (bottom right).

doi:10.1371/journal.pone.0158157.g001

infarct determined by the PET threshold for these animals were 2.96, 0.74, 2.30, 0.96, 0.97, and 0.80mL, giving an average grey matter infarct volume of 1.46 ± 0.38mL. 3 of the 6 animals that developed infarction required a second ET-1 injection to maintain depressed CBF in the ischemic territory.

The average relative CBF (rCBF normalized to contralateral grey matter) in the grey matter infarct region was calculated at each CTP imaging time point, for each animal. The average relative CBF value in the infarct regions over all animals and CTP imaging time points was 42 ± 16%. Fig 2 shows the average rCBF in the infarct region over time. On average, 60min after the 1st ET-1 injection rCBF dropped to ~40% and remained there for the duration of the experiment.

The infarct CBF histograms for each animal were normalized by scaling the number of infarct pixels in each bin up by the ratio of the total penumbra/oligemia pixels to the total infarct pixels (this scaling operation equalized the number of pixels in the infarct and penumbra/oligemia histograms). This normalization did not affect the ROC analysis because the relative frequencies of the CBF values were not changed, but it was necessary to prevent bias in the logistic regression caused by having a much greater number of pixels in the penumbra/oligemia group than in the infarct group. The CBF histograms for each animal can be found in the S1 Fig. Matlab was used to perform a binary logistic regression on the normalized histogram data for each animal. The probability of infarction predicted by logistic regression is plotted against CBF for each animal in Fig 3. The average of the 6 CBF values that corresponded to a 75% predicted probability of infarction in each animal was 4.5 ± 2.6 mL·min^{-1}·100g^{-1}.

Fig 4 shows the ROC curve for each animal. The average of the CBF values corresponding to the optimal operating points of the ROC curves [27] was 12.6 ± 2.8 mL·min^{-1}·100g^{-1}. The

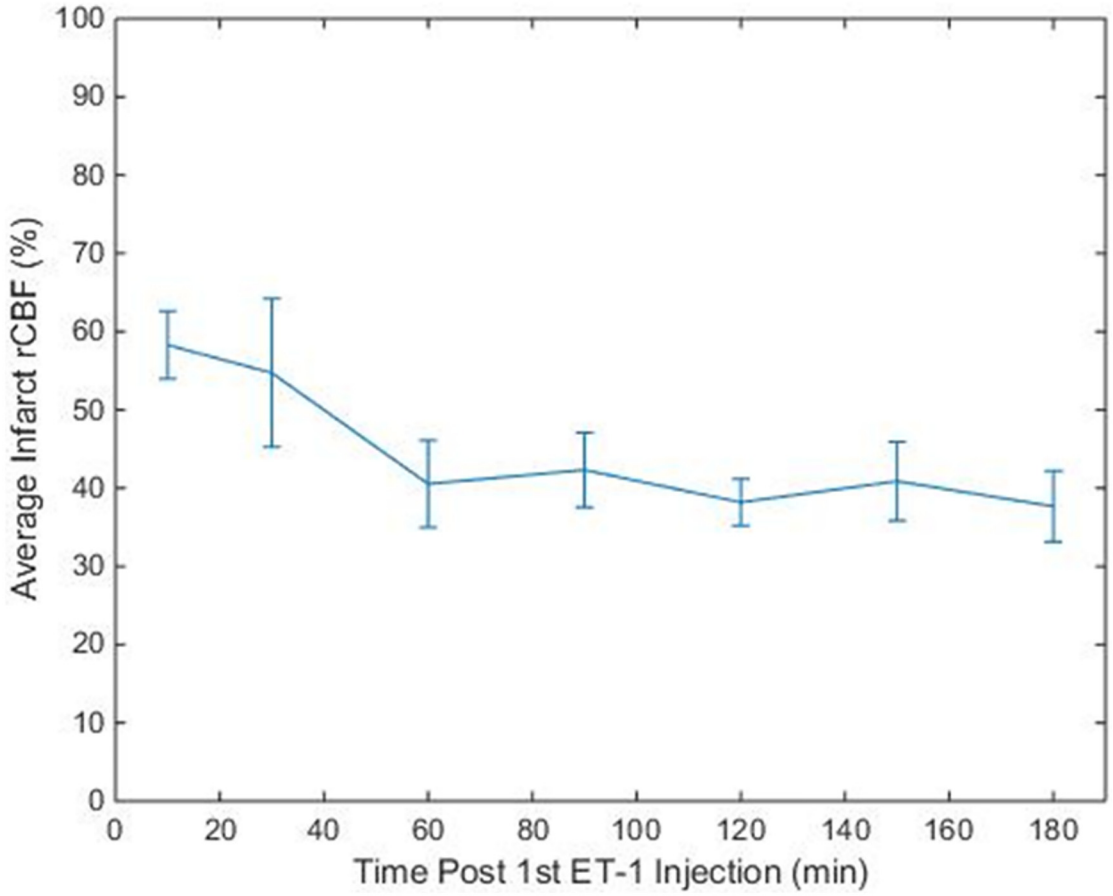

Fig 2. Average Relative CBF of Infarct ROIs. Average rCBF value from the infarct regions of the 6 animals at each time point. Error bars indicate standard error.

doi:10.1371/journal.pone.0158157.g002

sensitivity, specificity, and accuracy for infarct detection corresponding to the threshold in each animal, and the area under curve (AUC) can be found in Table 1.

Discussion

This study used a porcine model of ET-1 induced focal cerebral ischemia to determine a CTP-derived CBF threshold for infarction as determined by ^{18}F-FFMZ-PET imaging after 3 hours of ischemia. A threshold of 12.6 mL·min^{-1}·100g^{-1} was determined using ROC analysis. Previous animal studies have shown that the threshold for infarction is time dependent, dropping from 17–24 mL·min^{-1}·100g^{-1} for permanent occlusion to 12 mL·min^{-1}·100g^{-1} for occlusion lasting only 3 hours [20,28].

CTP-based time dependent thresholds for infarct core could be important for identifying late presenting or wake-up ischemic stroke patients that may still benefit from therapy [1]. Furthermore, time-dependent thresholds for infarction could be used to predict infarct growth in the time between admission imaging and reperfusion. This knowledge would be useful when deciding whether it is worthwhile to transfer a patient from a regional hospital to an IAT capable tertiary care hospital.

Prior perfusion threshold derivation studies could be affected by methodological problems. Many studies measure CBF during the acute phase of stroke, but do not determine the tissue

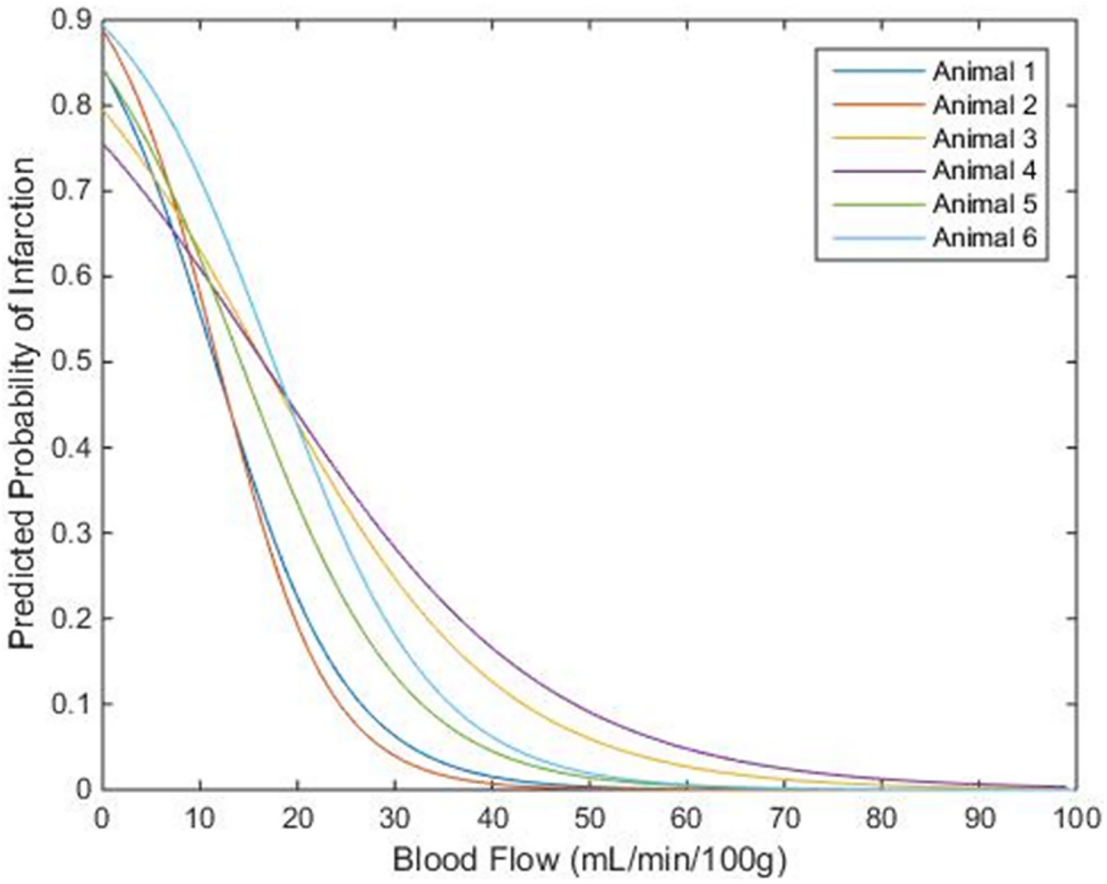

Fig 3. Predicted Probability of Infarction vs. CBF. Predicted probability of infarction from logistic regression plotted against CBF for each animal. The average of the CBF values that corresponded to a 75% predicted probability of infarction was approximately 4.5 ± 2.6 mL·min^{-1}·100g^{-1}.

doi:10.1371/journal.pone.0158157.g003

outcome until several days or even weeks later [3–5] introducing the uncertainty of infarct expansion in the interim. Furthermore, some studies use sub-optimal imaging data sets where the degree of reperfusion is not known [4]. With the experimental procedure used in this study CBF measurements and tissue outcome can be determined contemporaneously, eliminating the error caused by infarct expansion. This model also allows consistent monitoring of CBF using CTP, which gives information about the extent of reperfusion in the ischemic tissue.

The experimental model used in this study has several advantages over other animal models. The model used by Jones et al involved surgery to expose the MCA so it could be occluded using a ligature [28]. This is an example of a broader category of models which induce ischemia by occluding the MCA, generally using either an intra-arterial catheter [29] or by exposing the MCA and applying a clip or ligature [28]. Implementing these models of acute ischemia in pigs can be problematic for several reasons; the rete mirabelle makes it impossible to use an intra-arterial catheter [14], and using a clip or ligature requires very invasive surgical procedures such as an osteotomy on the orbital rim [15] or removal of an eye [16]. The ET-1 insult used in this study circumvents these difficulties since the only surgeries required are an incision on the scalp and a small burr hole in the skull (~2mm diameter). The less traumatic approach increases the ability to maintain the animal at its basal physiological state throughout the experiment. This is supported by the fact that in the Jones study 13 of the 33 monkeys had to be excluded from the

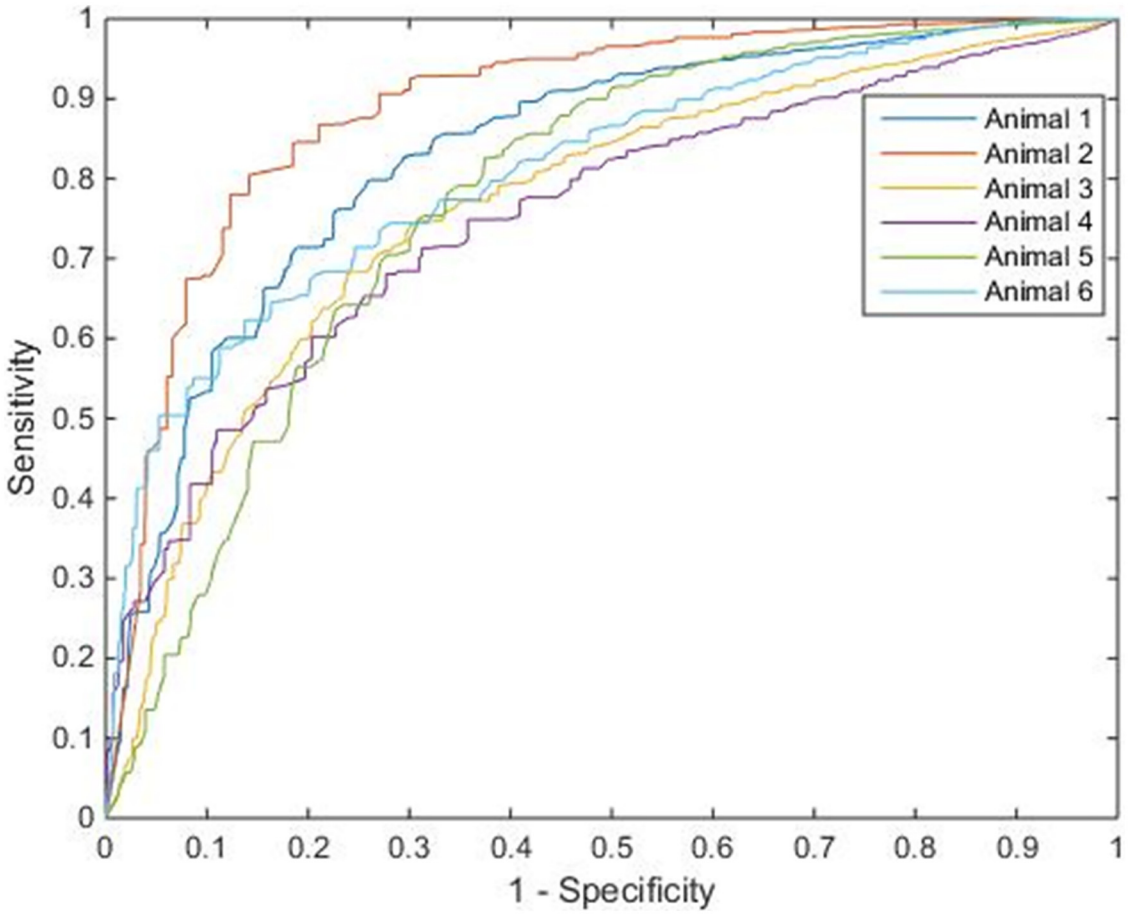

Fig 4. ROC Curve with Optimal Operating Point. ROC curves plotted for each of the 6 animals. Table 1 lists the CBF threshold derived from the optimal operating point of the ROC curve for each animal, and the corresponding sensitivity, specificity, accuracy, and AUC.

doi:10.1371/journal.pone.0158157.g004

data analysis because of subarachnoid hemorrhage, problems with the ligature or other technical issues [28] whereas in this study none of the 11 animals experienced these problems.

In animals 1, 2, and 6 the first dose, administered at the start of the experiment, was able to maintain rCBF in the final infarct region below 50% for most of the experiment. However, in animals 3, 4, and 5 the effect of the first dose was transient and a second dose was required. The

Table 1. ROC Parameters for Each Animal.

Animal	Threshold ($mL \cdot min^{-1} \cdot 100g^{-1}$)	Sensitivity	Specificity	Accuracy	Area Under Curve
1	10.1	0.80	0.74	0.77	0.8333
2	8.9	0.80	0.86	0.83	0.8908
3	15.0	0.74	0.70	0.72	0.7650
4	13.2	0.68	0.72	0.70	0.7528
5	12.1	0.75	0.69	0.72	0.7750
6	16.2	0.71	0.75	0.73	0.8110

The relevant parameters from the ROC analysis for each animal. The CBF threshold for infarction was the CBF value that corresponded to the optimal operating point of the ROC curve.

doi:10.1371/journal.pone.0158157.t001

second dose was given 90min after the first dose in animal 4 and 30min after the first dose in animal 5, the average rCBF for the remainder of the experiments dropped to ~37% and ~32% respectively in the final infarct regions. In animal 3, the second dose was given 90min into the experiment, causing a transient decrease in rCBF to 43% before it rose above 50% again 150min into the experiment. In this animal the second dose may have been given too late to counteract the reactive hyperemia associated with reperfusion [30,31]. There was some variation in response to ET-1 injections, but variation in CBF reduction is to be expected in animal models of stroke. In the study by Jones et al where cerebral ischemia was initiated in monkeys by ligating the MCA, the average CBF after ligation in the insular cortex was 17 ± 16 $mL \cdot min^{-1} \cdot 100g^{-1}$ [28], in this study the average CBF across all animals and time points after the first ET-1 injection was 15 ± 5 $mL \cdot min^{-1} \cdot 100g^{-1}$. On average rCBF in the final infarct tissue dropped to 56% for the first 30min of the experiment, from the 1hr time point until the end of the experiment rCBF was maintained at ~40%. Although the cerebral ischemia caused by ET-1 injections does not always replicate clinical cases of stroke, the model is still suitable for this study, where the objective is to cause a reduction in CBF leading to infarction, then determine a CBF threshold for distinguishing salvaged tissue from tissue which progressed to infarction.

Reperfusion and subsequent reactive hyperemia of the ischemic tissue after the first ET-1 injection is problematic in this model for several reasons. It can stop ischemic tissue from progressing to infarction, in these experiments 5 of 11 animals did not develop irreversible tissue damage, and the main reason for this was premature reperfusion of the ischemic tissue. When reperfusion occurs midway through the experiment it can be difficult to accurately define the ischemia duration. Lastly, some tissue progresses to infarction despite having a relatively high CBF at many time points during the experiment, either due to a weak response to the first injection or premature reperfusion and associated reactive hyperemia after the first injection wears off. This can result in high median CBF in the infarct regions leading to overestimation of the infarction threshold. For example, the average rCBF in the final infarct region for animal 6 was below 30% between the 30min and 120min time points and above 40% in the final 3 time points. It is possible that infarction was due to CBF dropping to an average value of 9.4 $mL \cdot min^{-1} \cdot 100g^{-1}$ for 30-90min in the middle of the experiment, and the higher CBF at the other time points resulted in an overestimated threshold of 16.2 $mL \cdot min^{-1} \cdot 100g^{-1}$ being derived. Using the median CBF value rather than the average CBF lessens the effect that reperfusion has on the derivation of a threshold.

In our experiments, reperfusion was partially mitigated by using semi-continuous CBF monitoring with CTP at 30min intervals to identify when reperfusion had started, so that another dose of ET-1 could be given. At each CTP imaging time point the CBF maps were calculated on a work station in the CT scanner suite within ~5-8min of completing the scanning, to monitor for reperfusion from the wearing off of the ET-1 effects. This method effectively limited reperfusion of the ischemic tissue, as the average rCBF in the final infarct region was below 50% for the duration of the experiment in 5 of 6 animals, and the average infarct rCBF across all animals and time points was 42 ± 16%.

Conclusions

The objective of this study was to determine a CBF threshold for infarction after 3 hours of ischemia. ROC analysis was used to find a threshold of 12.6 $mL \cdot min^{-1} \cdot 100g^{-1}$, which agrees well with the value of 12 $mL \cdot min^{-1} \cdot 100g^{-1}$ determined by Jones et al in 1981 [28]. The ET-1 model of acute stroke used in this study is easier to implement then other large animal stroke models. Despite some variation in response to ET-1 injections and instances of premature reperfusion, the model is comparable to other animal stroke models for the study objective.

Supporting Information

S1 Fig. Normalized frequency distributions for animals 1–6.
(TIF)

S2 Fig. Animal 1: PET image and CBF maps in slice with largest extent of infarct.
(TIF)

S3 Fig. Animal 2: PET image and CBF maps in slice with largest extent of infarct.
(TIF)

S4 Fig. Animal 3: PET image and CBF maps in slice with largest extent of infarct.
(TIF)

S5 Fig. Animal 4: PET image and CBF maps in slice with largest extent of infarct.
(TIF)

S6 Fig. Animal 5: PET image and CBF maps in slice with largest extent of infarct.
(TIF)

S7 Fig. Animal 6: PET image and CBF maps in slice with largest extent of infarct.
(TIF)

Acknowledgments

This study was partially supported by the Canadian Institute of Health Research and the Canadian Foundation for Innovation. The authors would like to thank Jennifer Hadway and Lise Desjardins for their assistance with handling the animals and the team working at the cyclotron at St. Joseph's Hospital for producing the ^{18}F-FFMZ for PET imaging.

Author Contributions

Conceived and designed the experiments: CD TL. Performed the experiments: EW CD LM TL. Analyzed the data: EW. Contributed reagents/materials/analysis tools: NC MK. Wrote the paper: EW LM. Edited and revised the manuscript: EW CD LM NC MK TL.

References

1. d'Esterre CD, Boesen ME, Hwan S, Pordeli P, Najm M, Minhas P, et al. Time-dependent computed tomographic perfusion thresholds for patients with acute ischemic stroke. Stroke. 2015; 46(12): 3390–3397. doi: 10.1161/STROKEAHA.115.009250 PMID: 26514186
2. Qiao Y, Zhu G, Patrie J, Xin W, Michel P, Eskandari A, et al. Optimal perfusion computed tomographic thresholds for ischemic core and penumbra are not time dependent in the clinically relevant time window. Stroke. 2014; 45(5): 1355–1362. doi: 10.1161/STROKEAHA.113.003362 PMID: 24627117
3. Murphy BD, Fox AJ, Lee DH, Sahlas DJ, Black SE, Hogan MJ, et al. Identification of penumbra and infarct in acute ischemic stroke using computed tomography perfusion-derived blood flow and blood volume measurements. Stroke. 2006; 37(7): 1771–1777. PMID: 16763182
4. Murphy BD, Fox AJ, Lee DH, Sahlas DJ, Black SE, Hogan MJ, et al. White matter thresholds for ischemic penumbra and infarct core in patients with acute stroke: CT perfusion study. Radiology. 2008; 247 (3): 818–825. doi: 10.1148/radiol.2473070551 PMID: 18424687
5. Bao DZ, Bao HY, Yao LZ, Pan YG, Zhu XR, Yang XS, et al. 64-slice spiral CT perfusion combined with vascular imaging of acute ischemic stroke for assessment of infarct core and penumbra. Exp Ther Med. 2013; 6(1): 133–139. PMID: 23935734
6. Pan J, Zhang J, Huang W, Cheng X, Ling Y, Dong Q, et al. Value of perfusion computed tomography in acute ischemic stroke: diagnosis of infarct core and penumbra. J Comput Assist Tomogr. 2013; 37(5): 645–649. doi: 10.1097/RCT.0b013e31829866fc PMID: 24045235

7. Eilaghi A, d'Esterre CD, Lee TY, Jakubovic R, Brooks J, Liu RTK, et al. Toward patient-tailored perfusion thresholds for prediction of stroke outcome. AJNR Am J Neuroradiol. 2014; 35(3): 472–477. doi: 10.3174/ajnr.A3740 PMID: 24113471
8. Yu Y, Han Q, Ding X, Chen Q, Ye K, Zhang S, et al. Defining core and penumbra in ischemic stroke: a voxel- and volume-based analysis of whole brain CT perfusion. Sci Rep. 2016; 10(6): 1–7.
9. Labeyrie MA, Turc G, Hess A, Hervo P, Mas JL, Meder JF, et al. Diffusion lesion reversal after thrombolysis: a MR correlate of early neurological improvement. Stroke. 2012; 43(11): 2986–2991. doi: 10.1161/STROKEAHA.112.661009 PMID: 22996954
10. Olivot JM, Mlynash M, Thijs VN, Purushotham A, Kemp S, Lansberg MG, et al. Relationships between cerebral perfusion and reversibility of acute diffusion lesions in DEFUSE: insights from RADAR. Stroke. 2009; 40(5): 1692–1697. doi: 10.1161/STROKEAHA.108.538082 PMID: 19299632
11. Freeman JW, Luby M, Merino JG, Latour LL, Auh S, Song SS, et al. Negative diffusion weighted imaging after IV tPA is rare and unlikely to indicated averted infarction. Stroke. 2013; 44(6): 1629–1634.
12. Heiss WD, Sobesky J, Smekal UV, Kracht LW, Lehnhardt FG, Thiel A, et al. Probability of cortical infarction predicted by flumazenil binding and diffusion-weighted imaging signal intensity: a comparative positron emission tomography/magnetic resonance imaging study in early ischemic stroke. Stroke. 2004; 35(8): 1892–1898. PMID: 15218157
13. Platt SR, Holmes SP, Howerth EW, Duberstein KJJ, Dove CR, Kinder HA, et al. Development and characterization of a Yucatan miniature biomedical pig permanent middle cerebral artery occlusion stroke model. Exp Transl Stroke Med. 2014; 6(1): 1–14.
14. Burbridge B, Matte G, Remedios A. Complex intracranial arterial anatomy in swine is unsuitable for cerebral infarction projects. Can Assoc Radiol J. 2004; 55(5): 326–329. PMID: 15646463
15. O'Brien MD, Waltz AG. Transorbital approach for occluding the middle cerebral artery without craniectomy. Stroke. 1973; 4(2): 201–206. PMID: 4702307
16. Imai H, Konno K, Nakamura M, Shimizu T, Kubota C, Seki K, et al. A new model of focal cerebral ischemia in the miniature pig. J Neurosurg. 2006; 104(2 Suppl): 123–132. PMID: 16506500
17. Nikolova S, Moyanova S, Hughes S, Bellyou-Camilleri M, Lee TY, Bartha R. Endothelin-1 induced MCAO: dose dependency of cerebral blood flow. J Neurosci Methods. 2009; 179(1): 22–28. doi: 10.1016/j.jneumeth.2009.01.009 PMID: 19428507
18. Virley D, Hadingham SJ, Roberts JC, Farnfield B, Elliot H, Whelan G, et al. A new primate model of focal stroke: endothelin-1-induced middle cerebral artery occlusion and reperfusion in the common marmoset. J Cereb Blood Flow Metab. 2004; 24(1): 24–41. PMID: 14688614
19. d'Esterre CD, Aviv RI, Morrison L, Fainardi E, Lee TY. Acute multi-modal neuroimaging in a porcine model of endothelin-1-induced cerebral ischemia: defining the acute infarct core. Transl Stroke Res. 2015; 6(3): 234–241. doi: 10.1007/s12975-015-0394-x PMID: 25876960
20. Hossmann KA. Viability thresholds and the penumbra of focal ischemia. Ann Neurol. 1994; 36(4): 557–565. PMID: 7944288
21. Sette G, Baron JC, Young AR, Miyazawa H, Tillet I, Barré L, et al. In vivo mapping of brain benzodiazepine receptor changes by positron emission tomography after focal ischemia in the anesthetized baboon. Stroke. 1993; 24(12): 2046–2058. PMID: 8248987
22. Heiss WD, Grond M, Thiel A, Ghaemi M, Sobesky J, Rudolf J, et al. Permanent cortical damage detected by flumazenil positron emission tomography in acute stroke. Stroke. 1998; 29(2): 454–461. PMID: 9472889
23. Gründer G, Siessmeier T, Lange-Asschenfeldt C, Vernaleken I, Buchholz HG, Stoeter P, et al. [^{18}F] Fluoroethylflumazenil: a novel tracer for PET imaging of human benzodiazepine receptors. Eur J Nucl Med. 2001; 28(10): 1463–1470. PMID: 11685488
24. Levêque P, Sanabria-Bohorquez S, Bol A, De Volder A, Labar D, Van Rijckevorsel K, et al. Quantification of human brain benzodiazepine receptors using [^{18}F]fluoroethylflumazenil: a first report in volunteers and epileptic patients. Eur J Nucl Med Mol Imaging. 2003; 30(12): 1630–1636. PMID: 13680197
25. Konstas AA, Goldmakher GV, Lee TY, Lev MH. Theoretic basis and technical implementations of CT perfusion in acute ischemic stroke, part 2: technical implementations. AJNR Am J Neuroradiol. 2009; 30(5): 885–892. doi: 10.3174/ajnr.A1492 PMID: 19299489
26. Richards JG, Möhler H, Schoch P, Häring P, Takacs B, Stähli C. The visualization of neuronal benzodiazepine receptors in the brain by autoradiography and immunohistochemistry. J Recept Res. 1984; 4 (1–6): 657–669. PMID: 6098675
27. Gallop RJ, Crits-Christoph P, Muenz LR, Tu XM. Determination and interpretation of the optimal operating point for ROC curves derived through generalized linear models. Understand Stat. 2003; 2(4): 219–242.

28. Jones TH, Morawetz RB, Crowell RM, Marcoux FW, FitzGibbon SJ, DeGirolami U, et al. Thresholds of focal cerebral ischemia in awake monkeys. J Neurosurg. 1981; 54(6): 773–782. PMID: 7241187

29. Van Winkle JA, Chen B, Lei IF, Pereira B, Raiput PS, Lyden PD. Concurrent middle cerebral artery occlusion and intra-arterial drug infusion via ipsilateral common carotid artery catheter in the rat. J Neurosci Methods. 2013; 213(1): 63–69. doi: 10.1016/j.jneumeth.2012.12.004 PMID: 23261656

30. Onetti Y, Dantas AP, Pérez B, Cugota R, Chamorro A, Planas AM, et al. Middle cerebral artery remodeling following transient brain ischemia is linked to early postischemic hyperemia: a target of uric acid treatment. Am J Physiol Heart Circ Physiol. 2015; 308(8): H862–H874. doi: 10.1152/ajpheart.00001.2015 PMID: 25637543

31. Traupe H, Kruse E, Heiss WD. Reperfusion of focal ischemia of varying duration: postischemic hyper- and hypo-perfusion. Stroke. 1982; 13(5): 615–622. PMID: 7123593